Nucleation of vortices inside open and blind microholes

A. Bezryadin*
Centre de Recherches sur les Très Basses Températures, Laboratoire associé à l'Université Joseph Fourier, CNRS, Boîte Postale 166, 38042 Grenoble-Cédex 9, France

Yu. N. Ovchinnikov
Landau Institute, Chernogolovka, 142432, Russia

B. Pannetier
Centre de Recherches sur les Très Basses Températures, Laboratoire associé à l'Université Joseph Fourier, CNRS, Boîte Postale 166, 38042 Grenoble-Cédex 9, France

(Received 2 June 1995)

The critical field of a thin superconducting film with a blind circular hole is found theoretically. It is shown that the value of the critical field is sensitive to the bottom thickness, but the orbital momentum, i.e., the number of vortices which nucleate inside the hole, is not sensitive. A simple boundary condition for a steplike thin film is derived and used for comparative numerical analysis of the superconductivity nucleation in a microdisk and near the hole. By increasing the thickness of the bottom of a blind hole one can transform the hole into a disk of the same radius which rests on top of the film. We show that such transformation leads to a jump in the number of vortices which nucleate at the critical magnetic field inside the perimeter of the hole (the disk). We report also the results of the Bitter decoration experiments of a thin superconducting film with a lattice of open or blind holes. It is found (in accordance with the calculation) that the bottom thickness has only a weak influence on the number of vortices captured by a hole during the cooling of the sample at a constant perpendicular magnetic field. All the experimental results are explained under the assumption that the vortices nucleated inside a hole rest inside during the cooling process and no additional vortices enter the hole.

I. INTRODUCTION

The critical field ($H_{c_3}^*$) near an open circular hole in a thin film or, what is very similar, near an empty cylindrical channel in a three-dimensional (3D) superconductor has been considered theoretically[1,2] and measured experimentally[3] (here and below we assume that the applied magnetic field is parallel to the axis of the hole). It was shown that the ratio $H_{c_3}^*/H_{c_2} = 1$ when $R \to 0$ and $H_{c_3}^*/H_{c_2} = 1.695$ when $R \to \infty$. Here R is the hole (or channel) radius and H_{c_2} is the upper critical field of a nonperforated infinite sample. The case $R \to \infty$ corresponds to the usual effect of surface superconductivity.[4] Due to the multiply connected geometry of the perforated sample, $H_{c_3}^*/H_{c_2}$ is an oscillating function with cusps of the hole area (more exactly it is a function of the magnetic flux in the hole: $\phi = \pi R^2 H$). The cusps appear when the number of vortices which nucleate inside the hole at $H_{c_3}^*$ increases by one, as in the Little-Parks effect.

Generally speaking, the effects of surface superconductivity are important at strong fields ($H \sim H_{c_2}$) because in such a case the superconducting order parameter is much higher near the hole edge than far from the hole in the uniform film. Such modulation of the order parameter modifies qualitatively the vortex pinning by an array of empty channels[5] or columnar defects. Also it gives rise to a type of surface barrier:[6,7] to approach and enter a hole a probe vortex must suppress superconductivity near the hole edge where the order parameter has a strong maximum (when $H \sim H_{c_2}$). Therefore the vortex should be repulsed from the hole. At last an overlap of the edge superconducting states localized near neighboring holes leads to formation of an array of Josephson junctions of superconducting–normal-metal–superconducting type with a unique coherence length in the whole system[3] (it is assumed here that the holes are organized in a periodic lattice).

In the present work we consider a more general case of a hole with a bottom (blind hole). It is assumed that this bottom is a part of the same film. Strictly speaking, in such a case, there is no hole in the film but only a hollow, so the sample is simply connected. Nevertheless it is shown that the critical field is qualitatively identical to that one of the film with a real hole. The amplitude of the ratio $H_{c_3}^*/H_{c_2}$ is decreased by the presence of the bottom but the positions of cusps are almost the same. The last statement means that the number of vortices which nucleate inside a blind hole (even inside a very shallow one) is approximately equal to this number for an open hole. Note that the density (experimental and theoretical) of fluxoids inside a hole is considerably higher than in the uniform film and the ratio can be as big as 4.

The present work has also a practical importance which is explained below. The vortex distribution in artificial perforated structures can be visualized by the Bitter decoration. For example the influence of the frustration on the vortex superlattice in a superconducting wire network has been studied by using this technique.[8] Usually the magnetic decoration can be done only at very low temperatures, when the screening effects are strong. At the same time it is assumed

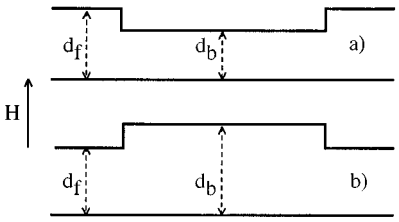

FIG. 1. Two simple configurations of the sample when the surface superconductivity effect can be observed. (a) Superconducting film with a blind hole (or a hollow); (b) disk which rests on a thin film. Magnetic field H is perpendicular to the film but parallel to the vertical parts of the sample surface inside the hole or at the edge of the disk.

(and argued in many cases[9]) that a kind of a "freezing effect" takes place, so the vortex superlattice, once determined at the critical temperature, is not changed during the subsequent cooling (note that in the present paper we discuss only field-cooling experiments). A direct Bitter decoration of artificial systems with holes is a difficult problem: vortices captured inside holes have a very small magnetic contrast. A powerful method which can be used for visualization of such vortices (or equivalently the vortices in unit cells of superconducting wire networks) consists of keeping a thin superconducting layer (the bottom) under the sample (the "flux compression" method).[7] This method is especially useful for observations of multiquanta vortices. Consider, for example, a hole with two vortices. By the usual "planarization" method[8] they cannot be resolved. On the contrary, if the hole has a superconducting bottom, then at low enough temperature these two vortices will be separated and visualized by the magnetic decoration as two independent spots (Fig. 4). From the above discussion it follows that for interpretation of the results obtained by the "flux compression," it is necessary to know how the presence of the bottom changes the vortex distribution at the nucleation temperature. In the present paper we consider in detail one particular case, the blind circular hole, and show that the bottom changes very weakly the number of vortices which nucleate in it.

II. CRITICAL FIELD OF A BLIND HOLE

Let us consider a circular blind hole of radius R with a bottom of thickness d_b in a film of thickness d_f exposed to a perpendicular magnetic field H [the cross section is shown in Fig. 1(a)]. Here we find the critical field of such system as a function of temperature and the bottom thickness. The problem is solved in the dirty limit in the full temperature range. For an arbitrary electron mean free path the result is valid in the temperature range close to the T_{c_0} (T_{c_0} is the critical temperature at zero field) and for $R \gg \xi(0)$ [the coherence length $\xi(0)$ is determined by the relation: $H_{c_2}(T) = \phi_0 / 2\pi\xi^2(T)$]. In such a case the order parameter ($\tilde{\Delta}$) satisfies at the superconducting transition the simple linear equation:[10]

$$-\left(\frac{\partial}{\partial \vec{r}} - 2ie\vec{A}\right)^2 \tilde{\Delta} = 2\lambda\tilde{\Delta}. \tag{1}$$

We set $\hbar = c = 1$. The proper value λ is proportional to the second critical field in the nonperforated infinite film: $\lambda = eH_{c_2}(T)$ and it is considered here as a given function of the temperature (T). We use the usual boundary condition for all points of the sample surface:

$$\vec{n}\left(\frac{\partial}{\partial \vec{r}} - 2ie\vec{A}\right)\tilde{\Delta} = 0, \tag{2}$$

where $\vec{n}$ is a vector normal to the surface. Let us consider the problem to be a three-dimensional one. At the critical field the superconducting state has an axial symmetry: $\tilde{\Delta}(\rho,\theta,z) = \Delta(\rho,z)e^{in\theta}$. Then in cylindrical coordinates (ρ,θ,z) one can write the equation for $\Delta(\rho,z)$

$$\left[-\frac{1}{\rho}\frac{\partial}{\partial\rho}\left(\rho\frac{\partial}{\partial\rho}\right) + \frac{n^2}{\rho^2} - \frac{\partial^2}{\partial z^2} + (eH\rho)^2 - 2eHn\right]\Delta = 2\lambda\Delta. \tag{3}$$

The function $\Delta(\rho,z)$ can be developed outside the hole in the following way: $\Delta_f = \Sigma_N f_N(\rho)\cos(k_N z)$ where the functions $f_N(\rho)$ satisfies the equation

$$\left[-\frac{1}{\rho}\frac{\partial}{\partial\rho}\left(\rho\frac{\partial}{\partial\rho}\right) + \frac{n^2}{\rho^2} + k_N^2 + (eH\rho)^2 - 2eHn\right]f_N = 2\lambda f_N, \tag{4}$$

and $k_N = \pi N/d_f$, $N = 0,1,2\ \ldots$. Consequently the solution for Δ_f, which is finite when $\rho \to \infty$, can be written as

$$\Delta_f(y,z) = \frac{1}{\sqrt{y}}\sum_N C_N W_{n/2+\lambda_{f_N}/2eH,n/2}(y)\cos\left(\frac{\pi N}{d_f}z\right), \qquad y > eHR^2, \tag{5}$$

where $y \equiv eH\rho^2$, C_N are some constants, $\lambda_{f_N} = \lambda - (1/2)(\pi N/d_f)^2$, and $W_{a,b}(y)$ is the Witteker function.[11] In the same way one can get the solution in the bottom of the hole:

$$\Delta_b(y,z) = \frac{1}{\sqrt{y}}\sum_N A_N M_{n/2+\lambda_{bN}/2eH,n/2}(y)\cos\left(\frac{\pi N}{d_b}z\right), \qquad y < eHR^2, \tag{6}$$

where $\lambda_{bN} = \lambda - (1/2)(\pi N/d_b)^2$ and the function W is replaced by the other linearly independent Witteker function M which is finite at the origin which coincides with the center of the hole.

The critical field of our system will be the field H_0 at which the solution given by (5) and (6) and its first derivative are continuous on the surface given by conditions $\rho = R$, $0 < z < d_b$ [in other points the functions (5) and (6) are always continuous]. Also the boundary condition (2) should be fulfilled on the surface: $\rho = R$, $d_b < z < d_f$ [in other points of the sample surface it is always true if one use the solution in the form (5) and (6)]. The orbital momentum n should be

chosen to obtain the maximum value of the critical field. The condition of the continuity of the order parameter on the surface $\rho = R$, $0<z<d_b$ is

$$\sum_{N_1=0}^{\infty} C_{N_1} W_{n/2+\lambda_{fN_1}/2eH,n/2}(eHR^2)\cos\left(\frac{\pi N_1}{d_f}z\right) \quad (N_1=0,1,2\ldots)$$
$$= \sum_{N=0}^{\infty} A_N M_{n/2+\lambda_{bN}/2eH,n/2}(eHR^2)\cos\left(\frac{\pi N}{d_b}z\right),$$

which should be fulfilled at any z from the interval $0<z<d_b$. It gives us the first pair of main equations:

$$A_0 M_{n/2+\lambda/2eH;n/2}(eHR^2) = \sum_{N_1=0}^{\infty} C_{N_1}\frac{d_f}{\pi N_1 d_b}\sin\left(\frac{\pi N_1 d_b}{d_f}\right) \times W_{n/2+\lambda_{fN_1}/2eH;n/2}(eHR^2), \quad (7)$$

$$A_{N\neq 0} M_{n/2+\lambda_{bN}/2eH;n/2}(eHR^2) = -\sum_{N_1=0}^{\infty} C_{N_1}\frac{2N_1 d_b}{\pi d_f}\frac{(-1)^N}{N^2-(N_1 d_b/d_f)^2}\sin\left(\frac{\pi N_1 d_b}{d_f}\right) \times W_{n/2+\lambda_{fN_1}/2eH;n/2}(eHR^2). \quad (8)$$

To obtain the Eq. (7) the above shown condition of the continuity of the order parameter has been integrated over z in the interval $0<z<d_b$. To obtain Eq. (8) the continuity condition has been multiplied by a factor $\cos[(\pi N/d_b)z]$ and then integrated in the same way.

The boundary condition (2) and the continuity of the derivative can be written in the form

$$\left.\frac{\partial[\Delta_f(y,z)]}{\partial y}\right|_{y=eHR^2} = \begin{cases} 0, & d_b<z<d_f \\ \left.\dfrac{\partial[\Delta_b(y,z)]}{\partial y}\right|_{y=eHR^2}, & 0<z<d_b. \end{cases}$$

It gives [if one takes into account the development (5) and (6)] the second couple of main equations:

$$C_0\left(\frac{1}{\sqrt{y}}W_{n/2+\lambda/2eH;n/2}(y)\right)'_y\Big|_{y=eHR^2} = \frac{d_b}{d_f}A_0\left(\frac{1}{\sqrt{y}}M_{n/2+\lambda/2eH;n/2}(y)\right)'_y\Big|_{y=eHR^2}. \quad (9)$$

(Note that we use the following notation for the derivative: $F'_y \equiv dF/dy$),

$$C_{N\neq 0}\left(\frac{1}{\sqrt{y}}W_{n/2+\lambda_{fN}/2eH;n/2}(y)\right)'_y\Big|_{y=eHR^2} = -\sum_{N_1=0}^{\infty} A_{N_1}\frac{2N}{\pi}\frac{(-1)^{N_1}(d_b/d_f)^2\sin(\pi N d_b/d_f)}{N_1^2-(N d_b/d_f)^2} \times\left(\frac{1}{\sqrt{y}}M_{n/2+\lambda_{bN_1}/2eH;n/2}(y)\right)'_y\Big|_{y=eHR^2}. \quad (10)$$

For the derivation of Eqs. (9) and (10) we have used the procedure analogous to Eqs. (7) and (8). The only difference was the interval $0<z<d_f$ of the integration and the factor $\cos[(\pi N/d_f)z]$

In principle the system of Eqs. (7), (8), (9), and (10) is complete and gives as a solution the ratio of the critical field near a hole $H^*_{c_3}$ and the bulk second critical field H_{c_2}: $H^*_{c_3}/H_{c_2} = eH_0/\lambda$ [here H_0 is the solution of the system (7), (8), (9), (10)]. It is a linear system of equations for unknown parameters A_N and C_N and it has nontrivial solutions only if

$$\det[\hat{E}-\hat{K}(y)]|_{y=eHR^2}=0. \quad (11)$$

In fact to derive Eq. (11) one has to exclude A_N and C_N constants in the set of Eqs. (7)–(10). In (11) $E_{ik}=\delta_{ik}$ is the unit matrix and the coefficients of the $\hat{K}$ matrix are the following:

$$\hat{K}_{00} = \hat{M}_{n/2+\lambda/2eH;n/2}(y)\left\{\frac{d_b}{d_f}\hat{W}_{n/2+\lambda/2eH;n/2}(y) + \frac{2d_f}{\pi^2 d_b}\sum_{N=1}^{\infty}\frac{1}{N^2}\sin^2\left(\frac{\pi N d_b}{d_f}\right)\hat{W}_{n/2+\lambda_{fN}/2eH;n/2}(y)\right\},$$

$$\hat{K}_{0N} = -(-1)^N\frac{2d_b}{\pi^2 d_f}\sum_{N_1=1}^{\infty}\sin^2\left(\frac{\pi N_1 d_b}{d_f}\right)\frac{\hat{W}_{n/2+\lambda_{fN_1}/2eH;n/2}(y)\hat{M}_{n/2+\lambda_{bN}/2eH;n/2}(y)}{N^2-(N_1 d_b/d_f)^2},$$

$$\hat{K}_{NM} = (-1)^{N+M}\frac{4}{\pi^2}\left(\frac{d_b}{d_f}\right)^3\sum_{N_1=1}^{\infty}\left\{\sin^2\left(\frac{\pi N_1 d_b}{d_f}\right)[N^2-(N_1 d_b/d_f)^2]^{-1}[M^2-(N_1 d_b/d_f)^2]^{-1} \times\hat{W}_{n/2+\lambda_{fN_1}/2eH;n/2}(y)\hat{M}_{n/2+\lambda_{bM}/2eH;n/2}(y)\right\},$$

where the definitions used are

$$\hat{M}_{a,b}(y)=\frac{[(1/\sqrt{y}M_{a,b}(y)]'_y}{\frac{1}{\sqrt{y}}M_{a,b}(y)}$$

and

$$\hat{W}_{a,b}(y)=\frac{(1/\sqrt{y})W_{a,b}(y)}{[(1/\sqrt{y})W_{a,b}(y)]'_y}.$$

Finally the critical field of the system under consideration is given by the single equation (11).

III. THIN-FILM LIMIT

The general equation (11) can be simplified if we assume that $d_f \ll \xi$, $d_b \ll \xi$ (the ratio d_b/d_f can be arbitrary; the coherence length is $\xi \equiv \sqrt{1/2\lambda}$). In this case all elements K_{0N} $(N \neq 0)$ are small and in the main approximation one can write

$$1=K_{00}, \tag{12}$$

if also $d_b \ll d_f$ then one can find the equation for the critical field in the first approximation

$$1=K_{00}+\sum_{N=1}^{\infty}\hat{K}_{N0}\hat{K}_{0N}. \tag{13}$$

In fact the perturbation theory is possible in all orders. In the case $d_b \ll \xi$ one can use the following asymptotic relation:

$$\hat{M}_{n/2+\lambda_{bN}/2eH;n/2}(y)=\left[2\sqrt{eHy}\left(\frac{d_b}{\pi N}\right)\right]^{-1}, \quad N>0.$$

Similarly if $d_f \ll \xi$, then

$$\hat{W}_{n/2+\lambda_{fN}/2eH;n/2}(y)=-2\sqrt{eHy}\left(\frac{d_f}{\pi N}\right), \quad N>0.$$

Now if $d_f \ll \xi$, $d_b \ll \xi$, and $d_b \ll d_f$ Eq. (13) can be rewritten

$$\left.\frac{(1/\sqrt{y})M_{n/2+\lambda/2eH;n/2}(y)}{[(1/\sqrt{y})M_{n/2+\lambda/2eH;n/2}(y)]'_y}\right|_{y=eHR^2}$$
$$=\frac{d_b}{d_f}\left.\frac{(1/\sqrt{y})W_{n/2+\lambda/2eH;n/2}(y)}{[(1/\sqrt{y})W_{n/2+\lambda/2eH;n/2}(y)]'_y}\right|_{y=eHR^2}$$
$$-\frac{4\sqrt{eHy}d_b}{\pi}\left[\frac{3}{2}+\ln\left(\frac{d_f}{2\pi d_b}\right)-\sum_{N=1}^{\infty}Nf^2(N)\right], \tag{14}$$

where the coefficient before the square brackets is small (proportional to d_b/ξ). The function $f(N)$ is given by

$$f(N)=\frac{1}{\pi^2}\int_0^{\infty}\frac{dx}{x}\frac{1-e^{-2\pi x}}{x^2+N^2}.$$

For large values of N one can get $f(N) = (1/\pi^2N^2) \times[C+\ln(2\pi N)]$ where $C = 0.5772\ldots$ is the Euler constant. Numerical calculation gives for the value of the sum in the Eq. (14)

$$\sum_{N=1}^{\infty}Nf^2(N)=0.0854\ldots .$$

We have used also by derivation of Eq. (14) the equation

$$\sum_{N=1}^{\infty}\frac{1}{N^3}\sin^2(\alpha N)=\frac{3\alpha^2}{2}+\alpha^2\ln\left(\frac{1}{2\alpha}\right),$$

which is valid for $\alpha \ll 1$.

Let us assume now that the film has a constant thickness (d) everywhere except some curve (boundary curve) where it has a stepwise change. For the blind hole such a curve is the perimeter of the hole where the thickness jumps from d_b to d_f. We will show firstly that in the general case the averaged value of the order parameter $\tilde{\psi}(\rho,\theta) = (1/d)\int_0^d\tilde{\Delta}(\rho,\theta,z)dz$, which is a two-dimensional function, satisfies the two-dimensional linear equation (1) everywhere except the hole perimeter. After we will derive simple boundary conditions for the order parameter $\tilde{\psi}(\rho,\theta)$ at the hole perimeter. These conditions are general and will be used to find the critical field of a disk and of a linear step on the film surface. The critical field in all such systems is higher than H_{c_2}. Note that the present discussion is valid only if the field is perpendicular to the film plane.

Let us consider an averaged over the film thickness order parameter: $\tilde{\psi}(\rho,\theta) = (1/d)\int_0^d\tilde{\Delta}(\rho,\theta,z)dz$ where d is equal either to d_b (inside the hole) or d_f (outside the hole). It is clear that such a function satisfies the 2D linear equation (1). Really if we make averaging over z of the left and right parts of the 3D equation (1) we get

$$-\frac{1}{d}\int_0^d\frac{\partial^2\tilde{\Delta}}{\partial z^2}dz-\left(\frac{\partial}{\partial\vec{\rho}}-2ie\vec{A}\right)^2\frac{1}{d}\int_0^d\tilde{\Delta}(\vec{\rho},z)dz$$
$$=2\lambda\frac{1}{d}\int_0^d\tilde{\Delta}(\vec{\rho},z)dz,$$

where $\vec{\rho}$ is the radius vector in the plane of the film. Note also that $\vec{A}$ is perpendicular to the z axis. The first term is equal to zero due to the boundary condition (2) so we get

$$-\left(\frac{\partial}{\partial\vec{\rho}}-2ie\vec{A}\right)^2\tilde{\psi}(\vec{\rho})=2\lambda\tilde{\psi}(\vec{\rho}). \tag{15}$$

The boundary condition for the function $\tilde{\psi}(\rho,\varphi)$ in zero approximation in parameters $d_b/\xi(T)$, $d_f/\xi(T)$ (d_b/d_f can be arbitrary) follows from Eq. (12):

$$d_b\frac{\partial\tilde{\psi}_b}{\partial\rho}(\tilde{\psi}_b)^{-1}=d_f\frac{\partial\tilde{\psi}_f}{\partial\rho}(\tilde{\psi}_f)^{-1}. \tag{16}$$

One can get it also from Eq. (14) by neglecting the linear correction (the term with the square brackets). Physically this condition means that the derivative of the 2D (averaged over the film thickness) order parameter $\tilde{\psi}(\rho,\varphi)$ has a jump at the boundary curve (where the film thickness has a jump), while the order parameter itself is continuous. The continuity of $\tilde{\psi}(\rho,\varphi)$ follows from the developments (5) and (6) and from the condition of the continuity of the 3D order parameter $\tilde{\Delta}(\rho,\theta,z)$ on the surface $\rho = R$, $0<z<d_b$. The ratio of the

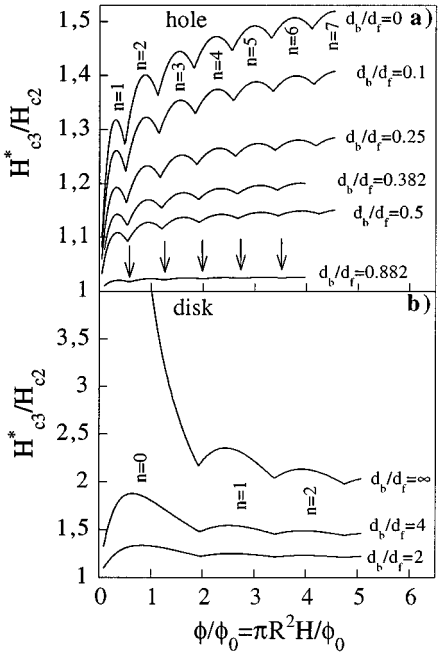

FIG. 2. The normalized critical field as a function of the reduced magnetic flux $\phi/\phi_0 = \pi R^2 H/\phi_0$ of the external field through the hole (the disk) area. Calculation is done under the assumption that d_b, $d_f \ll \xi(T^*_{c_3})$. (a) Critical field of blind holes with different values of the ratio between the bottom thickness d_b and the film thickness d_f [see the sample geometry in Fig. 1(a)]. Arrows show positions of cusps in the curve corresponding to $d_b/d_f = 0.882$. (b) Critical field of disks which rest on an infinite film [see the sample geometry in Fig. 1(b)].

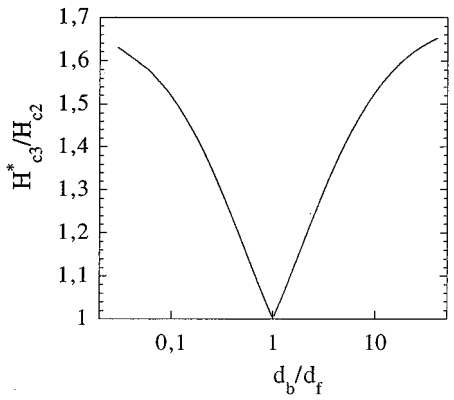

FIG. 3. Normalized critical field of a linear step on the film surface. The result is valid when the film thickness at both sides of the step is much smaller than the coherence length at the nucleation temperature.

derivatives is inversely proportional to the ratio of the thicknesses: $[d_b(\partial\tilde{\psi}_b/\partial\rho) - d_f(\partial\tilde{\psi}_f/\partial\rho)]_{\rho=R} = 0$. This condition should be fulfilled in all points of the stepwise increase of the film thickness, on the perimeter of the blind hole, for example. All numerical results of this paper are obtained using Eq. (15) and the condition (16). Note that Eq. (15) and the boundary condition (16) are true also in the case $d_b > d_f$ (the case of the disk). Only the following restriction is essential: $d_b, d_f \ll \xi$.

In Fig. 2(a) we present the normalized critical field [found numerically from (15) and (16)] of a blind hole versus the magnetic flux of the external field through its geometrical area. The same value for a disk is shown in Fig. 2(b) [the geometry of the sample and definitions are explained in Fig. 1(b)]. The increase of the bottom thickness d_b (or decrease of the disk thickness d_b) leads to a suppression of the surface superconductivity effect, but the number of vortices nucleated in the hole or in the disk is almost constant (this number is determined by cusp positions in the critical field curve). Numerical calculations show that the cusps corresponding to the same orbital number but to different values of the ratio d_b/d_f lie on a straight line (more exactly there are two different lines: for holes and for disks). When $d_b/d_f = 1$ the critical field is equal of course to H_{c_2} and the number of vortices inside a circle of radius R is undetermined (the last statement is true only exactly at the critical temperature), but single valued limits exist for the number of vortices inside the circle for $d_b/d_f \to 1-0$ and $d_b/d_f \to 1+0$. These two limits are different. An increase of d_b/d_f over unity leads to the transformation of the blind hole into a disk. This transition is accompanied by a jump in the orbital number which corresponds to an abrupt shift of cusps in the curves shown in Figs. 2(a) and 2(b). For example if $\phi/\phi_0 = 0.6$ then $n=2$ for holes with any value of the ratio d_b/d_f ($d_b < d_f$). In the case of disks ($d_b > d_f$) we find $n=0$ for the same value of the magnetic flux. A sufficient decrease of the temperature leads to formation of the Abrikosov lattice which is determined by the nonlinear term in the equation for the order parameter which is neglected in our consideration. Then the number of vortices is equal to the number of lattice knots inside the circle (in the limit $d_b \to d_f$). This number depends on the relative position of the vortex lattice and the circle (the perimeter of the hole or of the disk) and should be taken to give the minimum of the free energy. As a result we obtain different values for the number of vortices for the hole (maximum possible value) and for the disk (minimum possible value) in the limit $d_b \to d_f$. Note that in the uniform film ($d_b = d_f$) the number of vortices in a circle of a radius R averaged over the position of the circle center is equal naturally to the reduced magnetic flux $\phi/\phi_0 = \pi R^2 H/\phi_0$ of the external field through the hole (the disk) area as it is shown in Fig. 5c by the straight line ($\phi_0 = \pi\hbar c/e$ is the flux quantum).

Let us assume now that the hole radius is infinite ($R \to \infty$). In such a case, if $d_b \neq d_f$, our system becomes a thin film with a linear step on the surface. The height of this step is $|d_b - d_f|$. In this geometry d_b denotes the film thickness on one side of the linear step and d_f on the other side. To find the critical field near this linear step one can use the two-dimensional equation (15). Also if $d_b \ll \xi$ and $d_f \ll \xi$ then the boundary condition (16) is valid. Numerically we have found the reduced critical field shown in Fig. 3. In fact it is determined by the ratio of the thickness of two films d_b/d_f rather than by the step height $|d_b - d_f|$. Of course this is true only in the limit of zero film thickness. Note also that when the step height is small ($|d_b - d_f| \to 0$), the reduced critical field (more exactly the value $H_{c_3}/H_{c_2} - 1$) is proportional to the absolute value of the logarithm of the ratio d_b/d_f (Fig. 3). In the limit when one of the films is much thinner than the other ($d_b/d_f = 0$ or $d_b/d_f = \infty$) we come to the well-known result for the surface critical field: $H_{c_3}/H_{c_2} = 1.695$.

In fact any nonuniformity in the film thickness (but not only the discussed above sharp step on the film surface) leads to a local increase of the upper critical field. This phenomenon is especially important for ultrathin films, when the number of atomic layers is small. In this case even a monoatomic step on the surface leads to a considerable change of the ratio d_b/d_f and consequently of the critical field (which can be only increased in accordance with Fig. 3). An important consequence of such an increase is a maximum of the superconducting order parameter near the step which contributes to the vortex pinning. This contribution should be dominant at high fields ($H \approx H_{c_2}$) when the averaged order parameter and therefore the energy of the intervortex interaction is small far from the step. The strongest force acting on vortices in such a case is the repulsion from the maxima of the order parameter created by nonuniformities in the film thickness.

IV. BITTER DECORATION OF OPEN AND BLIND MICROHOLES

In the previous paragraph we have seen that the critical field (or the critical temperature in field-cooling experiments) of a film with a (blind) hole is an oscillatory dependence of the magnetic flux. Positions of the cusps in this dependence are unexpectedly stable to variations of the bottom thickness. A direct way to find experimentally the positions of the cusps could be, for example, a resistive measurement of the critical field or the critical temperature. It was done for an Al film but only with open holes.[3] Such measurements should be much more difficult in the case of blind holes, especially if the bottom thickness is almost equal to the film thickness, because in such a case the amplitude of the oscillation of the critical field should be very small [see Fig. 2(a)].

The positions of the cusps correspond to the moments when the number of vortices inside a hole (this number will be referred to as the ''filling factor'' FF) changes by one. An independent way to determine the filling factor versus the flux through the hole is the Bitter decoration which gives a possibility to visualize individual vortices in the sample. It is an indirect method because the decoration can be done only at low temperature when the applied field is much lower than the temperature-dependent critical field, while our theoretical results are concerned with the critical region ($H \rightarrow H^*_{c_3}$). At the same time it can be expected that the vortex distribution, once determined at the nucleation temperature, is not changed considerably during the cooling (we discuss here only field-cooling experiments). Therefore the number of vortices which we find at the low temperature inside a hole should be very close to the number of vortices which are nucleated into the hole at the critical temperature (this number is determined by the positions of the cusps on the critical field found in the previous paragraph, except probably small regions near the cusps themselves). It is a kind of ''freezing effect,'' argued and verified experimentally in Ref. 7. Without going into a detailed discussion, we can mention here that this effect is due to the small field [$H \propto 10$ Oe $\ll H_{c_1}(0)$] which means a weak repulsion between the vortices, quite strong intrinsic pinning in the Nb film, and the surface barrier due to the considerable enhancement of the order parameter near the hole edge. The last circumstance is important only at high temperatures, when the applied field is of the order of H_{c_2}. It should be mentioned also that if one or more vortices are captured inside a hole, then the external vortices should be repulsed by it due to the superconducting currents circulating near the hole edge.[12]

All the magnetic decorations are curried out after the sample, a thin perforated Nb film, has been cooled in a weak perpendicular field $H = 6.37$ Oe down to $T_{\rm dec} = 4.2$ K (note that $T_{\rm dec} \ll T_{c_0} = 9.2$ K). The Bitter decoration consists of the evaporation of a small amount of a ferromagnetic metal (60 μg of Ni in our case) not far from the sample surface. Precautions are taken to prevent any considerable heating of the sample. The Ni atoms form small monodomain particles ($\approx$ 200 Å) which are attracted to the centers of vortices due to the magnetic-field gradient. After the decoration the sample is warmed up to the room temperature. The positions of vortices are marked by attracted Ni particles and visible in the electron microscope as white spots (for more details see Refs. 7,8).

The holes are made by the reactive ion etching (RIE) of a Nb epitaxial film covered by PMMA electron-sensible resist which is patterned by the electron-beam lithography. An incomplete ion etching leads to formations of blind holes. The bottom thickness can be varied by changing the time of RIE. Experimentally we have used samples with open holes ($d_b = 0$), holes with a thin bottom ($d_b = 650$ Å), and holes with a very thick bottom ($d_b = 1500$ Å) which is almost equal to the film thickness ($d_b = 1700$ Å). The holes are organized in arrays. In each array there are about 50 identical holes which are forming a regular triangular lattice of period $a = 6.1$ μm. To sweep the magnetic flux ($\pi R^2 H$) we have available (on the same substrate) many arrays which differ from each other by the hole radius $0.15\ \mu\text{m} < R < 2.2\ \mu$m (the magnetic field is uniform and the same in all experiments).

The presence of a superconducting bottom inside holes gives a possibility to observe and count the captured vortices (Fig. 4). So far one can determine the filling factor (FF): the number of vortices trapped in a single hole. Its averaged value ($\langle \text{FF} \rangle$) can also be found because we have about 50 (or more) identical holes in each array.

Some experiments are done with open holes when the trapped vortices are not visible. In this case one can also determine $\langle \text{FF} \rangle$ as the difference between the density of vortices in a uniform nonperforated film and the density of noncaptured vortices in the film with holes. To find $\langle \text{FF} \rangle$ one should divide this difference by the density of holes. This method can give a considerable error if the period of the hole lattice is much larger than the averaged intervortex distance and, in addition, not all vortices are well recognized. The direct method which is possible with blind holes is much easier and more reliable. It enables us to distinguish definitely between trapped and nontrapped vortices in all cases, even when the bottom is very thick, because each hole is surrounded by a region which is practically free of vortices (Fig. 4).

The experimentally found filling factor $\langle \text{FF} \rangle$ is shown in Fig. 5 versus the magnetic flux of the external field through the hole area. Three types of symbols correspond to open holes (open circles), holes with a bottom of thickness $d_b = 650$ Å (crosses), and holes with a thick bottom d_b

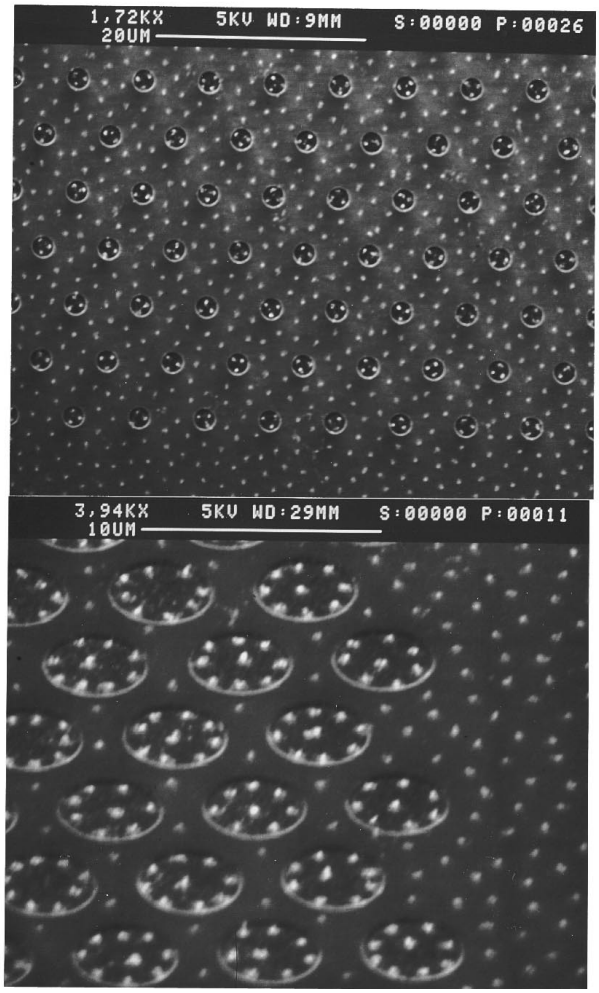

FIG. 4. Visualization of vortices (white spots) using the Bitter decoration and SEM. The decoration is fulfilled at $T = 4.2$ K after the sample has been cooled at a constant field $H = 6.37$ Oe. The period of the triangular lattice of circular holes is $a = 6.1$ μm, the bottom thickness is $d_b = 650$ Å. Each hole at the top picture ($R = 1$ μm) captures three vortices (except two or three holes). The vortex lattice outside holes is disordered. An increase of the hole radius leads to the trapping of the most of vortices (bottom picture, $R = 2.2$ μm). Inside holes the vortices are concentrated along the perimeter, except one which is in the center. Note that the bottom picture is a photo of an inclined sample.

$=1500$ Å (solid squares). The solid straight line denotes the vortex density in a nonperforated part of the film multiplied by the hole area. One can see that the density of fluxoids is considerably higher inside the holes, even if the bottom thickness is very close to the film thickness (solid squares). In accordance with the calculations of the previous paragraph it is found that the difference between experimental values of $\langle \mathrm{FF} \rangle$ corresponding to holes with different bottom thicknesses ($0 < d_b/d_f < 0.9$) is considerably smaller than the difference between those values and the vortex density (multiplied by the hole area) in the uniform film (straight line in Fig. 5). Theoretical values of the filling factor are shown by the stepwise lines in Fig. 5 for different values of the ratio d_b/d_f. They show the number of fluxoids which appear in the hole at the field-dependent critical temperature. This number is, in fact, the orbital number n (see the previous

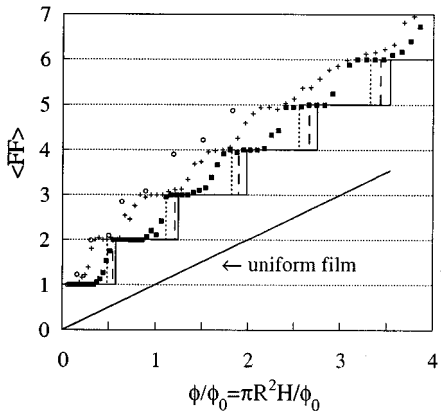

FIG. 5. Experimentally found filling factor, averaged over about 50 holes versus the magnetic flux in the hole. The open discs correspond to open holes ($d_b/d_f = 0$), crosses correspond to blind holes with $d_b/d_f \approx 0.38$, and solid squares correspond to very shallow blind holes with $d_b/d_f \approx 0.88$. Calculated value of the filling factor at the nucleation temperature is shown for open holes $d_b/d_f = 0$ (dotted line), and for blind holes with $d_b/d_f = 0.38$ (dashed line) and with $d_b/d_f = 0.88$ (stepwise solid line). The straight solid line is the averaged number of vortices in a uniform nonperforated film inside an imaginary circle of radius R.

paragraph) which maximizes the critical field. The jumps of the calculated filling factor correspond to the positions of the cusps of the critical field $H^*_{c_3}$ [Fig. 2(a)]. Finally we find that our simple model that the FF is constant with the temperature explains quite well the experimental data.

For more accurate description it is necessary to consider the region below the critical temperature. Numerical calculations show[13] that a decrease of the temperature in a constant field can cause a first-order phase transition with an increase by one in the orbital number of the superconducting state localized near the hole. Such transitions should be considered as an entrance of an additional vortex into the hole. They are possible only at high temperatures and lead to some increase of $\langle \mathrm{FF} \rangle$ with respect to its value at the nucleation temperature (Fig. 5).

The stepwise dependence of the averaged filling factor $\langle \mathrm{FF} \rangle$ is just a reflection of the fact that all holes contain exactly the same number of vortices. This fact naturally follows from the condition that the filling factor is constant during the field cooling because there is no doubt that the same number of vortices should be nucleated in two geometrically equivalent holes (if they are far apart from each other and therefore independent). The mentioned above first-order transitions should take place normally at the same temperature for all holes. On the contrary, if we neglect in our discussion the surface superconductivity effects and the strong enhancement of the order parameter near the hole edge, the explanation of the stepwise dependence of the averaged filling factor (Fig. 5) is not evident, especially if one takes into account that the experimental filling factor is much smaller than its expected equilibrium value[7] at $T_{\mathrm{dec}} = 4.2$ K.

V. CONCLUSIONS

We have calculated the critical field near a blind hole in a thin superconducting film. It is higher than the upper critical

field in a uniform nonperforated film but lower than in the film with an open hole. The orbital number (or the number of trapped vortices) which maximizes the critical field is practically the same for open and very shallow blind microholes. The same conclusion follows from the magnetic decoration experiments of a thin Nb film with open and blind holes. It is demonstrated that the presence of a superconducting layer (the bottom) inside holes gives a possibility to observe and count the captured vortices directly. It is found that in the field-cooling experiments even very shallow blind holes (hollows) have practically the same efficiency in vortex trapping as real open holes. The result is explained by taking into account the edge superconducting states characterized by the strong enhancement of the order parameter.

ACKNOWLEDGMENTS

This work was supported by the CEE ''SUPNET'' Contract No. ERBCGRCT920068. Yu. O. would like to express his gratitude to P. Monceau for hospitality and to the CNRS for the financial support.

*Present address: Delft University of Technology, Dept. of Applied Physics, P.O. Box 5046, 2600 GA Delft, The Netherlands.

[1] Yu.N. Ovchinnikov, Sov. Phys. JETP **52**, 755 (1980).
[2] A.I. Buzdin, Phys. Rev. B **47**, 11 416 (1993).
[3] A. Bezryadin and B. Pannetier, J. Low Temp. Phys. **98**, 251 (1995).
[4] P.G. de Gennes, *Superconductivity of Metals and Alloys* (Benjamin, New York, 1966).
[5] Yu.N. Ovchinnikov, Sov. Phys. JETP **52**, 923 (1980).
[6] A. Bezryadin, A. Buzdin, and B. Pannetier, in *Macroscopic Quantum Phenomena and Coherence in Superconducting Networks*, edited by C. Giovannella and M. Tinkham (World Scientific, Singapore, 1995).
[7] A. Bezryadin and B. Pannetier, J. Low Temp. Phys. **102**, 73 (1996).
[8] K. Runge and B. Pannetier, Europhys. Lett. **24**, 737 (1993).
[9] M. Giroud, O. Buisson, Y.Y. Wang, B. Pannetier, and D. Mailly, J. Low Temp. Phys. **87**, 683 (1992).
[10] E. Helfand and N.R. Werthamer, Phys. Rev. **147**, 288 (1966); Yu.N. Ovchinnikov, Sov. Phys. JETP **39**, 538 (1974).
[11] *Handbook of Mathematical Functions*, edited by M. Abramowitz and I.A. Stegun (Dover, New York, 1970), p. 504.
[12] G.S. Mkrtchyan and V.V. Shmidt, Sov. Phys. JETP **34**, 195 (1972).
[13] A. Bezryadin, A. Buzdin, and P. Pannetier, Phys. Rev. B **51**, 3718 (1995).